

# A Simple Combined Dynamic-Equilibrium Model of CO<sub>2</sub> Capture by a Pelleted Zeolite Sorbent<sup>\*</sup>

Luigi Bisone<sup>\*</sup> Sergio Bittanti<sup>\*\*</sup> Silvia Canevese<sup>\*\*\*</sup>  
Elahe Davarpanah<sup>\*\*\*\*</sup> Antonio De Marco<sup>\*</sup>  
Maurizio Notaro<sup>\*\*\*</sup> Valter Prandoni<sup>\*\*\*</sup>

<sup>\*</sup> Process scientist, Milan, Italy (e-mail: lbis@inwind.it, antoniodemarco65@gmail.com).

<sup>\*\*</sup> Politecnico di Milano, Milan, Italy, and CNR - The National Research Council of Italy (e-mail: sergio.bittanti@polimi.it)

<sup>\*\*\*</sup> RSE (Ricerca sul Sistema Energetico) S.p.A., Milan, Italy, (e-mail: {silviamaaria.canevese, maurizio.notaro, valter.prandoni}@rse-web.it)

<sup>\*\*\*\*</sup> Politecnico di Torino, Turin, Italy (e-mail: elahe.davarpanah@polito.it)

---

**Abstract:** Carbon dioxide (CO<sub>2</sub>) can be effectively captured from gas mixtures by adsorption on zeolite pellets in fixed-bed columns. In this paper we start from an experimental analysis of CO<sub>2</sub> adsorption on a sample of few pellets, to end up with a simulation model for an adsorption column filled with a large number of pellets. The initial experimental analysis is based on dedicated isothermal tests carried out with a gas adsorption analyzer. For the relation between the measured amount of adsorbed CO<sub>2</sub> per unit sorbent mass and the input adsorption pressure and temperature, an equilibrium Three-Site Langmuir (TSL) equation is here adopted. Its unknown parameters, namely the saturation capacities, the affinities and the adsorption energies, are estimated by minimizing the error between the equation and the measures. Then, for a whole adsorption column, a simple dynamic model is worked out, based on one-dimensional partial differential equations along the column axial direction: these account basically for mass and energy conservation, for the bulk gas flow and for the porous sorbent. The overall description obtained by combining the TSL equation with the rest of the model is validated against experimental tests, consisting of inlet CO<sub>2</sub> molar fraction steps, on a laboratory-scale column.

*Keywords:* Physical adsorption, dynamic model, carbon capture, solid sorbent, zeolite 13X, parameter identification, three-site Langmuir equilibrium model.

---

## 1. INTRODUCTION

Adsorption on solid sorbents is currently among the most effective technologies for carbon dioxide (CO<sub>2</sub>) separation from gas mixtures (Shi Y. (2017); Davarpanah (2020)). Significant applications include post-combustion capture from flue gases (Samanta et al. (2012); Sjoström and Krutka (2010)), as in coal-fired power plants, and pre-combustion capture, such as for biogas upgrade to biomethane (Kulkarni et al. (2018)). Solid sorbents are often preferred to liquid ones (like aqueous solutions of alkanolamines) because they involve less energy-intensive processes and are much less prone to volatility and corrosion (Davarpanah et al. (2020)); besides, they can exhibit large adsorption capacity and high gas adsorption rate. Synthetic zeolite 13X, in particular, which is commercially

available, is widely studied and it is sometimes adopted as a benchmark material, to compare CO<sub>2</sub> separation performance of new possible sorbents (Hu et al. (2014)). In this work, focus is on a dynamic model for a fixed-bed adsorption column filled with 13X pellets, to be employed for biomethane production from biogas. As a test case, a laboratory-scale column (Bisone et al. (2019)) located at RSE “Processes and catalytic materials” laboratory in Piacenza, Italy, is adopted (Section 2). The column has been conceived to study the upgrade of biogas obtained from anaerobic digestion of organic waste (with around 60% CH<sub>4</sub> and 40% CO<sub>2</sub> molar fractions), in particular to test the ability of the sorbent to reduce CO<sub>2</sub> molar fraction to 3% or even less, so that the obtained biomethane can be injected into the Italian natural gas network. However, since the interaction between the sorbent and CH<sub>4</sub> can be neglected, preliminary tests to study the interaction between the sorbent and CO<sub>2</sub> have been carried out with an N<sub>2</sub>/CO<sub>2</sub> mixture, instead of a CH<sub>4</sub>/CO<sub>2</sub> mixture.

To set up, first of all, an equilibrium model of adsorption of CO<sub>2</sub> on 13X pellets, isothermal data collected on a small sample of such pellets (Davarpanah (2020); Davarpanah

---

<sup>\*</sup> This work has been financed by the Research Fund for the Italian Electrical System in compliance with the Decree of Minister of Economic Development April 16, 2018. The support by Fondazione Politecnico di Milano and the National Research Council of Italy (CNR - IEIIT) is also gratefully acknowledged, together with the support by Politecnico di Torino.

et al. (2020)) are employed: these allow to fit a three-site Langmuir correlation between the adsorbed amount of CO<sub>2</sub> and pressure and temperature values (Section 3). Then, a dynamic description of mass and energy exchanges along the axial direction of a whole column is worked out and combined with the equilibrium chemical model (Section 4). The overall model thus obtained is validated against the mentioned tests on the lab-scale column, as illustrated in Section 5. Section 6 proposes some concluding remarks.

## 2. COLUMN DESCRIPTION AND OPERATION

The laboratory column is depicted schematically in Fig. 1. Its main geometrical and material parameters are collected in table 1 (Bisone et al. (2019); Davarpanah et al. (2020); GRACE Davison (2010)). It is a finned heat-exchanger tube, where the annulus sectors delimited by the fins form eight peripheral channels filled with the sorbent, which is made up of highly porous approximately spherical zeolite pellets. Gas mixtures flow across the eight parallel and independent channels, while a cooling/heating fluid, water here, flows through the central cylindrical channel, to control the sorbent temperature without direct contact with it. When exiting the tube, the fluid feeds an outer jacket, which is in series with respect to the channels and increases the surface for heat exchange with the sorbent.

Three thermocouples of type K (placed at the inlet, middle and outlet section) measure the sorbent temperature inside the column, while a continuous analyzer measures gas composition at the inlet and at the outlet. The thermal fluid temperature and flow rate are controlled by means of an external refrigerating/heating circulator, equipped with a circulating pump. For column depressurization in the sorbent regeneration stage, a vacuum pump is adopted.

The column operation for biogas upgrade is described in detail in Bisone et al. (2019). The column undergoes a batch process in a cyclic way, to be able to be coordinated and synchronized with other similar columns to obtain a continuous biomethane flow. The batch process is composed of different stages: adsorption, regeneration (desorption), cooling and idle status (Ruthven (1984)). The *adsorption stage* is carried out by keeping the thermal fluid at low temperature (25 °C) and with flow rate about 1320-1560 l/h, while injecting biogas into the column inlet. As biogas crosses the column sections, CO<sub>2</sub> is adsorbed on the sorbent inner porous surface. When CO<sub>2</sub> starts to exit the column (e.g. when its molar fraction measured at the column outlet reaches 1-2%), the *regeneration stage* is started. It consists of injecting a stripping inert gas (here N<sub>2</sub>) into the column outlet (i.e. countercurrent with respect to the previous biogas flow) and with a molar flow rate around 1/10 of the previous biogas molar flow rate, of depressurizing the column (to about 0.1 bar minimal pressure) by means of the vacuum pump and of heating the circulating thermal fluid (up to 85-90 °C). This stage is followed by the *cooling stage*, which includes stopping the vacuum pump and N<sub>2</sub> injection and cooling the thermal fluid. When the three measured temperatures approach the one set for adsorption (i.e. they reach 25 °C ± 2 °C), the column is set to the *idle state*, so it is ready for the next adsorption stage.

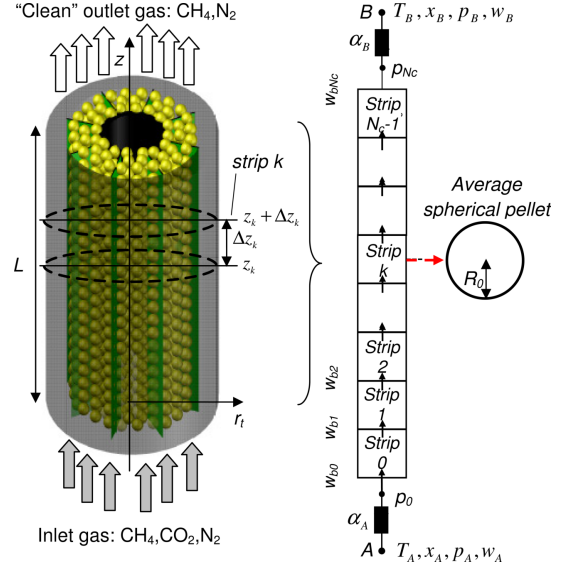


Fig. 1. Adsorption/desorption column structure and spatial discretization scheme for the model

## 3. EXPERIMENTAL ANALYSIS AND PARAMETER IDENTIFICATION

The adopted sorbent is commercial zeolite 13X (GRACE Davison (2010)), where a small quantity of an adsorptive clay binder is added to the zeolite crystals molecular sieve in order to extrude the material in the form of beads, or pellets (for comparison, for an analysis of binderless 13X adsorption properties, see e.g. Silva et al. (2012)). Each pellet is composed of a number of porous crystals with a grain size around 25 Å. The inter-crystalline pores are called mesopores while the pores inside each crystal are micropores. CO<sub>2</sub> can be assumed to enter the mesopores by diffusion and, in case of non-uniform distribution of mesopores, also via viscous flow. Transport from the mesopores to the micropores can instead be related to Knudsen's diffusion (Do (1998)). On the micropore inner surface, physical adsorption/desorption occurs (Ruthven (1984)). To describe this phenomenon, it is customary to introduce a variable, called  $\theta$ , defined as

$$\theta := \frac{n_{ads}/M_s}{\phi A_{act,s}/M_s} = \frac{n_{ads}/M_s}{n_{max}/M_s}, \quad (1)$$

where  $n_{max} := \phi A_{act,s}$ , with  $\phi$  [mol/m<sup>2</sup>] the amount of active sites available for CO<sub>2</sub> per unit surface and  $A_{act,s}$  the

Table 1. Lab-scale column: geometric and pellet parameters

Parameter	Symbol	Value
Length	$L$	0.97 m
Cross section area	$A$	$0.9695 \cdot 10^{-3} \text{ m}^2$
Column inner radius	$R_{in}$	0.012 m
Column outer radius	$R_{ext}$	0.0225 m
Sorbent mass	$M_s$	0.589 kg
Pellet radius	$R_0$	0.0015 m
Pellet mass density	$\rho_p$	1390 kg/m <sup>3</sup>
Bulk mass density	$\rho_s$	626 kg/m <sup>3</sup>
Bulk void fraction	$\varepsilon_b$	0.5526
Pellet void fraction	$\varepsilon_p$	0.4
Pore diameter	$d_p$	7.5 Å
Cubic grain side	$L_{cr}$	24.74 Å
Heat capacity	$c_s$	960 J/(kg · K)

sorbent active surface area.  $n_{max}/M_s$  [mol/kg] is the sorbent adsorption capacity per unit mass, i.e. the maximum number of moles which 1 kg of sorbent can adsorb up to its saturation, i.e. the number of moles of available active sites per sorbent kg.  $n_{ads}/M_s$  [mol/kg] is the number of moles actually adsorbed by 1 kg of sorbent in the current operating conditions. In order to characterize  $n_{ads}$ , and therefore  $\theta$ , in equilibrium conditions first of all, we resort to gas adsorption measurements, as explained below.

Gas adsorption measurements are typically used to characterize the porous structure of a solid porous adsorbent including the dimension and distribution of the pores, their surface area and total volume (for the considered zeolite 13X, see Davarpanah et al. (2020); moreover, by the energy-dispersive X-ray (EDX) technique, the same study indicates that the total number of cations present on the surface of zeolite 13X is around 5.29 mol/kg). Through this analysis the adsorption performance of the adsorbent material is also obtained, in terms of mol adsorbed per kg adsorbent. The measurements can be performed on various types of gas and vapor such as  $N_2$ ,  $CO_2$ ,  $CH_4$  and  $H_2O$ . In this work, the physical adsorption of gas molecules onto the surface of the adsorbent has been measured by means of a Quantachrome Autosorb-iQ instrument (manometric or volumetric gas adsorption analyzer). The set-up (Fig. 2) is composed of two cells: a dosing cell (with a known pressure) and a sample cell, connected by a valve. The measurements have been carried out by introducing 4 pellets of zeolite 13X with an average diameter of 3 mm into the uptake cell. Initially the sample is degassed at 300 °C under vacuum and a set of pressure values (at equilibrium) is inserted into the program. The measurement starts by injecting small amounts of  $CO_2$  and monitoring the pressure until arriving to the desired equilibrium value. This process is repeated until achieving the final pressure. The incremental dosing to access the micropore analysis for this instrument is in the range of  $10^{-6} - 10^{-7}$  for  $p_f/P_0$ , where  $p_f$  is the adsorbate pressure and  $P_0 = 760$  Torr. Starting from  $p_f$  pressure values the instrument computes the adsorbed moles/kg of sorbent and supplies them up to the sixth decimal point. A sample is considered to have reached equilibrium when the pressure between two readings changes less than 0.0008 atm.

Here, the isotherms are measured at three temperatures, namely 10, 30 and 50 °C (i.e. 283.15 K, 303.15 K and 323.15 K), for each of which sixteen equilibrium pressure values up to 100 kPa are adopted: in total,  $N_t = 48$  experimental points are available. The steady-state isotherm experimental data are shown in Fig. 3. Such data are now employed to estimate the uncertain parameters (Bittanti (2019)) of a model for the equilibrium adsorbed  $CO_2$ . More precisely, a Three-Site Langmuir (TSL) model (Son et al. (2018)) is adopted, which describes, at steady state, the moles of adsorbed  $CO_2$  per unit sorbent mass, as

$$\frac{n_{ads}}{M_s} = \sum_{j=1}^3 \frac{a_j b_j p_f}{1 + b_j p_f}, a_j = a_{0j} + \frac{c_{0j}}{T_s}, b_j = b_{0j} e^{\frac{E_j}{RT_s}}, \quad (2)$$

where  $T_s$  is the sorbent temperature and  $R$  the gas constant. The  $a_j$ s [mol/kg] are the saturation capacity parameters, whose dependency on temperature is expressed by parameters  $c_{0j}$ s (here the  $c_{0j}$ s are assumed to be equal to zero); the  $b_{0j}$ s [ $Pa^{-1}$ ] are the affinity parameters and each

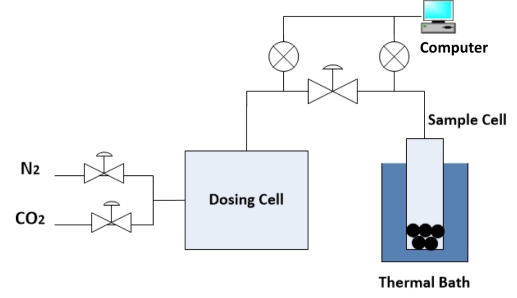


Fig. 2. Brunauer-Emmett-Teller instrument schematic

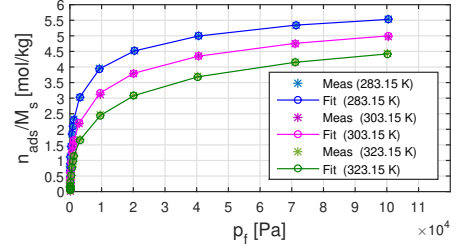


Fig. 3. Fitted TSL model versus measured adsorption data

$E_j$  [J/mol] is the adsorption energy of the single adsorbate. This model also yields that

$$\frac{n_{max}}{M_s} = \sum_{j=1}^3 a_j. \quad (3)$$

To estimate the unknown parameters in model (2), we minimize the quadratic error between the values of  $n_{ads}/M_s$  obtained from the model and the measured data  $n_{ads,meas}/M_s$  in all the experiments (Son et al. (2018)):

$$ERR = \sum_{N=1}^{N_t} (n_{ads}(N)/M_s - n_{ads,meas}(N)/M_s)^2. \quad (4)$$

By using, to this purpose, the *fminsearch* built-in routine in Matlab<sup>®</sup>, the following values for the model parameters are obtained:  $a_{01} = 2.78$  mol/kg,  $a_{02} = 1.42$  mol/kg,  $a_{03} = 2.02$  mol/kg,  $b_{01} = 1.35 \cdot 10^{-10}$  Pa<sup>-1</sup>,  $b_{02} = 2.53 \cdot 10^{-10}$  Pa<sup>-1</sup>,  $b_{03} = 4.23 \cdot 10^{-11}$  Pa<sup>-1</sup>,  $E_1 = 35025.81$  J/mol,  $E_2 = 41920.57$  J/mol,  $E_3 = 31043.07$  J/mol; here, adopting zero  $c_{0j}$ s yields a better fit than assuming nonzero  $c_{0j}$ s. The obtained fit is compared with the measured data in Fig. 3, which shows a very good agreement (the fit and the data are almost indistinguishable).

The model just identified will be included in the overall column dynamic model described in the following.

#### 4. COLUMN MODEL

We recall that pellets here fill the column outer channels, where the gas mixtures are injected (into the column inlet for adsorption and into the column outlet for desorption). Thus, for modelling purposes, two control volumes are considered (Bisone et al. (2017); Bisone et al. (2019)): the bulk volume, consisting of the interstices among the pellets in the sorbent bed, and the sorbent volume itself with mesopores and micropores. Since preliminary tests with the lab-scale column are with  $CO_2/N_2$  mixtures only, in the column dynamic model the inlet gas mixture is assumed to be composed of  $CO_2$  and  $N_2$  only. In the model

the adsorption of  $N_2$  is neglected, because  $N_2$  is an inert and is not being adsorbed.

The proposed model includes one-dimensional Partial Differential Equations (PDEs), for mass and energy conservation along the column axial spatial coordinate  $z$ . Note that we have made some simplifying assumptions. To be precise, we have assumed that, along the column radial direction  $r_t$ , there is a uniform average behaviour. Moreover, for adsorption inside the porous pellets, we have adopted an equilibrium adsorption model, as already hinted at. Besides, since the measured overall pressure drop is about 5000 Pa, pressure in the model is considered to be uniform throughout the column (although it can be variable with time; indeed, its dynamics depend mainly on the volumes of the manifolds between which the column is inserted, see Fig. 1 on the right and Bisone et al. (2017)).

#### 4.1 Fluid-Dynamic Model in the Bulk Gas Volume

Let  $w_b$  be the bulk gas molar flow rate,  $\rho$  the bulk gas molar density,  $\varepsilon_b$  the bulk void fraction,  $x_{b,CO_2}$   $CO_2$  molar fraction in the bulk gas, and  $w'_{l,CO_2}$  what we call  $CO_2$  ‘‘lateral’’ molar flow rate per unit length, i.e. the molar flow rate which is adsorbed by the pellets per unit length of the column. Along the column bulk, the mass conservation equation for  $CO_2$  and the global mass conservation equation read as

$$\frac{\partial \rho A \varepsilon_b x_{b,CO_2}}{\partial t} + \frac{\partial w_b x_{b,CO_2}}{\partial z} = -w'_{l,CO_2} \quad (5)$$

$$\frac{\partial \rho A \varepsilon_b}{\partial t} + \frac{\partial w_b}{\partial z} = -w'_{l,CO_2}. \quad (6)$$

By means of equation (6) and by defining

$$y := -\ln(1 - x_{b,CO_2}), \quad (7)$$

equation (5) can be rewritten as

$$\rho A \varepsilon_b \frac{\partial y}{\partial t} + w_b \frac{\partial y}{\partial z} = -w'_{l,CO_2}. \quad (8)$$

In a quasi-steady-state assumption and by assuming uniform pressure, equation (6) becomes

$$\frac{\partial w_b}{\partial z} = -w'_{l,CO_2}. \quad (9)$$

In order to compute  $w'_{l,CO_2}$ , a pellet model is introduced; this also includes the model of the crystals in the pellet, as described below.

#### 4.2 Fluid-Dynamic and Kinetic Model in the Sorbent

Let us consider the sorbent volume, which is composed of the pellets. The lateral molar flow rate between the bulk and the sorbent, namely  $w'_{l,CO_2}$ , has to describe the transport of  $CO_2$  from the bulk to the micropores, so it has to take into account also the presence of the binder, beside that of the zeolite crystals. Here, a quasi-steady-state assumption is made, by neglecting the dynamics related to accumulation of  $CO_2$  in the sorbent empty volumes. Thus, letting  $C_{b,CO_2} = \rho x_{b,CO_2}$  and  $C_p$  be  $CO_2$  molar concentration in the bulk gas and in the sorbent micropores respectively, one can write

$$w'_{l,CO_2} = \tilde{\sigma}_k (C_{b,CO_2} - C_p) \quad (10)$$

$$\tilde{\sigma}_k := \frac{A_{pr} N_{cr} N_p}{L} \frac{\sigma_{k,bn,pr} \sigma_{k,bn}}{\sigma_{k,bn} + \sigma_{k,bn,pr}}, \quad (11)$$

where  $A_{pr}$  is the cross-section area of the micropores in a crystal,  $N_{cr}$  is the number of crystals in a pellet and  $N_p$  is the number of pellets in the column.  $\sigma_{k,bn}$  is the conductance between the bulk and the binder/mesopores and  $\sigma_{k,bn,pr}$  the conductance between the binder/mesopores and the crystal micropores:

$$\sigma_{k,bn,pr} = D_K / (L_{cr}/2), \quad (12)$$

$$\sigma_{k,bn} = 12\pi R_0 \varepsilon_{bn} D_{bn} / (A_{pr} N_{cr}), \quad (13)$$

where  $D_K = 48.5 d_p \sqrt{T_s/44}$  is  $CO_2$  Knudsen diffusion coefficient in the micropores,  $D_{bn}$  is the diffusion coefficient in the binder and in the mesopores,  $\varepsilon_{bn}$  is the void fraction of the binder and of the mesopores. In (13) no viscous flow appears, since its contribution can be neglected, as one can verify by considering laminar flow across the mesopores and the binder, with Kozeny coefficient  $\kappa = L_{cr}^2 \varepsilon_p^3 / [(1 - \varepsilon_p)^2 150\mu]$  and pressure  $p = 100$  kPa, and, e.g.,  $D_{bn}$  associated to binary diffusion of  $CO_2$  in  $N_2$ . Bulk-pellet conductance  $\tilde{\sigma}_k$  is an uncertain parameter; in it  $\sigma_{k,bn}$  is the most important contribution and it is also highly uncertain. If the mesoporous structure of the sorbent and the binder structure were known,  $\sigma_{k,bn}$  could be identified accurately. In this work, we have identified  $\sigma_{k,bn}$  by trial and error during model simulation, by assuming for  $D_{bn}$  a value of the same order of magnitude of binary diffusion.

We also recall that  $w'_{l,CO_2}$  is due to adsorption, so it can be related to the  $\theta$  variable as

$$w'_{l,CO_2} = \frac{\phi A_{act} N_{cr} N_p}{L} \frac{\partial \theta}{\partial t}, \quad (14)$$

where  $A_{act}$  is the active surface of a crystal. Of course,  $\phi A_{act} N_{cr} N_p = \phi A_{act,s} = n_{max}$ . Here,  $n_{max}$  is estimated by using (3); the obtained value is slightly larger than the measured number of cations on the surface: this appears to be consistent with the fact that some active sites can adsorb more than one  $CO_2$  molecule (Stevens et al. (2008)).

#### 4.3 Thermal Model

A simplified thermal model is adopted for the column, by assuming that the metal walls temperature is a known input (indeed, it is kept under control by the cooling/heating system) and by neglecting the dynamics of the bulk gas temperature; therefore, the energy conservation equation in the sorbent only is written, as

$$\frac{4}{3}\pi R_0^3 \rho_p c_s \frac{N_p}{L} \frac{\partial T_s}{\partial t} = H_m \frac{\phi A_{act,s}}{L} \frac{\partial \theta}{\partial t} - L_m \gamma_{s,m} (T_s - T_m), \quad (15)$$

where  $T_s$  [K] is the sorbent temperature,  $T_m$  [K] the metal wall temperature,  $c_s$  [J/(kg·K)] the sorbent specific heat,  $H_m$  [J/mol]  $CO_2$  adsorption heat,  $\gamma_{s,m}$  [W/(m<sup>2</sup>·K)] the heat transfer coefficient between the sorbent and the heating/cooling system metal wall,  $L_m$  [m] the metal wall equivalent exchange perimeter (Bisone et al. (2019)).

#### 4.4 Adsorption Model

For  $CO_2$  adsorption on the micropores active surface, one can assume, for simplicity, that equilibrium between  $CO_2$  in the micropores and the adsorbed  $CO_2$  is reached instantly. Therefore, an algebraic correlation between  $C_p$  and  $\theta$  is adopted in this work (for a dynamic model,

instead, see e.g. Won et al. (2012), where a combination of a linear and a quadratic driving force is implemented). More precisely, we resort to the mentioned TSL model (Son et al. (2018)) for the equilibrium adsorbed CO<sub>2</sub>. Since CO<sub>2</sub> is not the only species in the gas mixture,  $p_f$  is replaced with CO<sub>2</sub> partial pressure  $C_p RT_s$ ; thus,

$$\theta = \frac{1}{\sum_{j=1}^3 a_j} \sum_{j=1}^3 \frac{a_j b_j C_p RT_s}{1 + b_j C_p RT_s} := f(C_p, T_s). \quad (16)$$

To include this part of the model in the overall column model, the following relation is adopted:

$$\frac{\partial \theta}{\partial t} = \frac{\partial f}{\partial C_p} \frac{\partial C_p}{\partial t} + \frac{\partial f}{\partial T_s} \frac{\partial T_s}{\partial t}. \quad (17)$$

*Remark:* An estimate of the adsorption heat for CO<sub>2</sub> can be obtained by replacing the TSL model into the Clausius-Clapeyron equation (Son et al. (2018)):

$$H_m = - \frac{\sum_{j=1}^3 \left[ R \frac{c_{0j} b_j}{1 + b_j C_p RT_s} + E_j \frac{a_j b_j}{(1 + b_j C_p RT_s)^2} \right]}{\sum_{j=1}^3 \frac{a_j b_j}{(1 + b_j C_p RT_s)^2}}. \quad (18)$$

For the experimental conditions considered in the simulations (Section 5), this appears to be consistent with experimental values (in the 42-50 MJ/kmol range at ambient temperature) reported in Davarpanah et al. (2020). Therefore, this estimate is included in the thermal model.

#### 4.5 Overall Column Model and Numerical Solution

On the whole, we consider a non-linear PDE model, composed of equations (8), (9) (together with definition (7)), (10), (14), (15), and also (17) which is obtained from the equilibrium kinetic model expressed by (16). In the simulations (Section 5), the model initial condition is the steady-state operating point characterized by clean sorbent and a constant known N<sub>2</sub> molar flow rate (no CO<sub>2</sub>) flowing across the clean column, so  $\theta(z, t = 0) = 0$  and  $x_{b,CO_2}(z, t = 0) = 0, \forall z$ . Starting from such an initial condition, we impose, as a boundary condition, a step variation to CO<sub>2</sub> molar fraction at the column inlet, while keeping the total molar flow rate at the inlet constant ( $w_b = w_{b0} = const$ , which is the molar flow rate for  $z = 0$ ).

In order to find a numerical solution for each  $(z, t)$ , we divide the range of  $z$  into  $N_c$  elementary intervals, here called *strips*, each of which with length  $\Delta z = L/N_c$ . Therefore, a set of nonlinear Ordinary Differential Equations (ODEs) is obtained from the PDEs for each strip, and the outlet  $y$  variable of each strip is adopted as the input at the inlet of the following strip. The ODEs in each strip are solved by using the *ode15s* built-in routine in Matlab<sup>®</sup>.

### 5. MODEL VALIDATION

A set of adsorption tests has been carried out on the lab-scale column, with the N<sub>2</sub>/CO<sub>2</sub> inlet gas mixture characterized by pressure  $p = 100$  kPa, molar flow rate  $w_b = 287$  NI/h ( $3.545 \cdot 10^{-3}$  mol/s), temperature around 293 K (21.5 °C) or 313 K (40.6 °C); such temperature values have also been set as the temperature setpoint for the circulating bath. In these conditions, CO<sub>2</sub> molar fraction steps have been given at the column inlet:  $x_{b,CO_2}(z = 0, t)$  around 5%, 10%, 20% or 40%. Such tests have been simulated by adopting  $N_c = 194$  strips (so each strip is 5 mm long).

Coefficient  $\bar{\sigma}_k$  has been adjusted by trial and error to  $3.457 \cdot 10^{-3}$  m<sup>2</sup>/s, a value which has been taken as a constant in all our simulations, and  $L_m \gamma_{s,m}$  to 23.011 W/(m · K).

Measured and simulated values are compared in Fig. 4 and Fig. 5: for each test, the bulk CO<sub>2</sub> molar fraction at the column outlet and the sorbent temperature at the column inlet and outlet. As to the temperature at the inlet, due to uncertainty on the actual position of the thermocouple along coordinate  $z$ , the simulated value reported is the mean of the values obtained for the first three strips; similarly for the temperature at the outlet. From the various diagrams one can notice rather good agreement between the model and the experiment, except in some cases for the outlet temperature and for the outlet molar fraction exiting delay for the two highest molar fractions at 293 K. Such discrepancies can be related to the very simple model adopted for the sorbent control volume and for the temperature dynamics.

### 6. CONCLUSION

The main parameters characterizing equilibrium conditions for CO<sub>2</sub> adsorption on zeolite 13X spherical pellets have been identified from *ad-hoc* experimental tests on few pellets. The identified equilibrium model has been integrated within a first-principle dynamic model of a fixed-bed tubular column filled with many pellets. The overall model has been validated thanks to step tests on a lab-scale column. This validation is a remarkable outcome considering the simplicity of the model adopted in this paper. However, the column thermal model (including also the temperature control system) has to be refined and a deeper insight has to be taken into how adsorption occurs inside the crystals distributed in the pellets, so mass, momentum and energy conservation equations along the spherical pellet radial direction have to be included in the model. Further research activities include reconsidering the identification phase to better estimate the chemical kinetics parameters, also due to the presence of other components in the feedgas mixture, e.g. residual humidity (Joos et al. (2013); Li et al. (2009)).

### REFERENCES

- Bisone, L., Bittanti, S., Canevese, S., Davarpanah, E., De Marco, A., Notaro, M., and Prandoni, V. (2019). Model-based design of a control system for the upgrade of biogas with zeolite sorbent reactors. In *18<sup>th</sup> European Control Conference (ECC)*, 1188–1194.
- Bisone, L., Bittanti, S., Canevese, S., De Marco, A., and Prandoni, V. (2017). Cyclic automation of a plant for the removal of CO<sub>2</sub> from biogas. *IFAC-PapersOnLine*, 50(1), 10802–10807. 20<sup>th</sup> IFAC World Congress.
- Bittanti, S. (2019). *Model Identification and Data Analysis*. John Wiley & Sons, Inc., Hoboken, NJ, USA.
- Davarpanah, E. (2020). *Investigation and Modelling of Porous Solid Sorbents and Bio-based Ionic Solvents for the Separation of CO<sub>2</sub> from Flue Gas*. PhD thesis, Politecnico di Torino, Turin, Italy.
- Davarpanah, E., Armandi, M., Hernández, S., Fino, D., Arletti, R., Bensaid, S., and Piumetti, M. (2020). CO<sub>2</sub> capture on natural zeolite clinoptilolite: Effect of temperature and role of the adsorption sites. *J. Environ. Manage.*, 275, 111229.

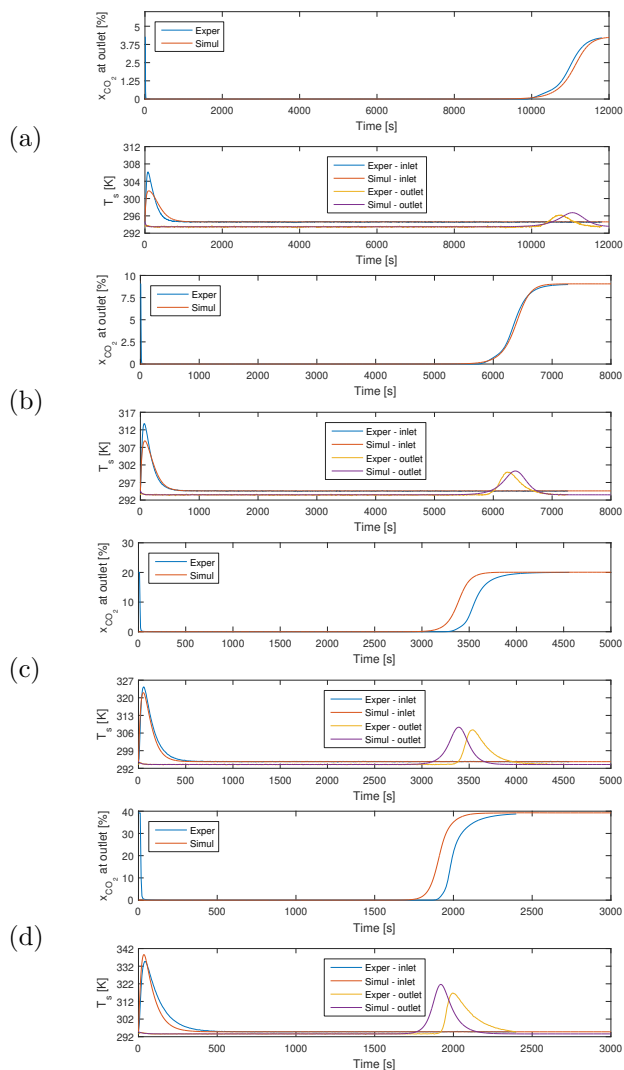


Fig. 4. Simulation versus experimental results for the lab-scale column, for (a) 5%, (b) 10%, (c) 20%, (d) 40% inlet  $\text{CO}_2$  molar fraction and temperature 293 K

- Do, D.D. (1998). *Adsorption Analysis: Equilibria and Kinetics*. Published by Imperial College Press and distributed by World Scientific Publishing Co.
- GRACE Davison (2010). SYLOBEAD<sup>®</sup> - Adsorbents for process applications. URL <https://grace.com/>.
- Hu, X., Mangano, E., Friedrich, D., Ahn, H., and Brandani, S. (2014). Diffusion mechanism of  $\text{CO}_2$  in 13X zeolite beads. *Adsorption*, 20(1), 121–135.
- Joos, L., Swisher, J.A., and Smit, B. (2013). Molecular simulation study of the competitive adsorption of  $\text{H}_2\text{O}$  and  $\text{CO}_2$  in zeolite 13X. *Langmuir*, 29(51), 15936–15942.
- Kulkarni, B., Kasikamphaiboon, P., and Khunjan, U. (2018).  $\text{CO}_2$  adsorption from biogas using amine-functionalized  $\text{MgO}$ . *Int. J. Chem. Eng.*, 1–9.
- Li, G., Xiao, P., Webley, P.A., Zhang, J., and Singh, R. (2009). Competition of  $\text{CO}_2/\text{H}_2\text{O}$  in adsorption based  $\text{CO}_2$  capture. *Energy Procedia*, 1(1), 1123–1130. Greenhouse Gas Control Technologies 9.
- Ruthven, D.M. (1984). *Principles of Adsorption and Adsorption Processes*. John Wiley & Sons, NY, USA.
- Samanta, A., Zhao, A., Shimizu, G., Sakar, P., and Gupta, R. (2012). Post-combustion  $\text{CO}_2$  capture using solid sorbents: a review. *I. & E. C. Research*, 51, 1438–1463.

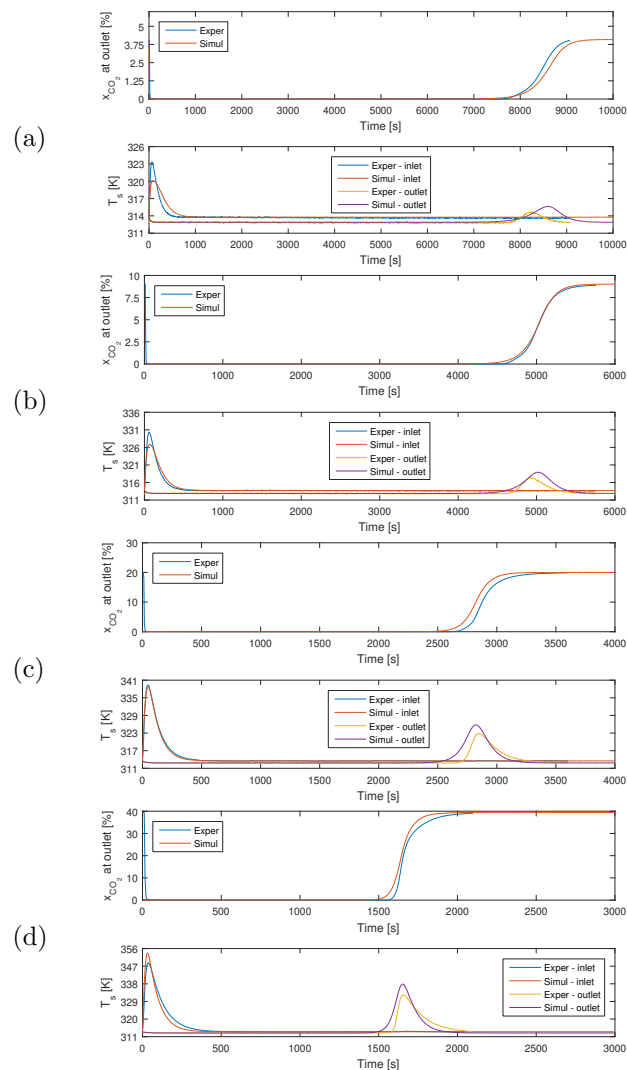


Fig. 5. Simulation versus experimental results for the lab-scale column, for (a) 5%, (b) 10%, (c) 20%, (d) 40% inlet  $\text{CO}_2$  molar fraction and temperature 313 K

- Shi Y., Liu Q., H.Y. (2017).  $\text{CO}_2$  capture using solid sorbents. In W.Y. Chen, T. Suzuki, and M. Lackner (eds.), *Handbook of Climate Change Mitigation and Adaptation*, 2349–2404. Springer, Cham.
- Silva, J.A., Schumann, K., and Rodrigues, A.E. (2012). Sorption and kinetics of  $\text{CO}_2$  and  $\text{CH}_4$  in binderless beads of 13X zeolite. *Micropor. Mesopor. Mat.*, 158, 219–228.
- Sjostrom, S. and Krutka, H. (2010). Evaluation of solid sorbents as a retrofit technology for  $\text{CO}_2$  capture. *Fuel*, 89, 1298–1306.
- Son, K.N., Cmarik, G.E., Knox, J.C., Weibel, J.A., and Garimella, S.V. (2018). Measurement and prediction of the heat of adsorption and equilibrium concentration of  $\text{CO}_2$  on zeolite 13X. *JCED*, 63(5), 1663–1674.
- Stevens, R.W., Siriwardane, R.V., and Logan, J. (2008). In situ Fourier Transform Infrared (FTIR) investigation of  $\text{CO}_2$  adsorption onto zeolite materials. *Energy & Fuels*, 22(5), 3070–3079.
- Won, W., Lee, S., and Lee, K.S. (2012). Modeling and parameter estimation for a fixed-bed adsorption process for  $\text{CO}_2$  capture using zeolite 13X. *Sep. Purif. Technol.*, 85, 120–129.